ORIGINAL RESEARCH PAPER

Removal of Methylene Blue Using Polyacrylic Acid/Octavinyl Polyhedral Oligomeric Silsesquioxane Nanocomposite

Mansoureh Zarezadeh-Mehrizi [1], Majid Karimi [1]*, Zahra Kalantari khoramdareh [1], Mahnaz Qomi [2, 3]

[1] Polymerization Engineering Department, Iran Polymer and Petrochemical Institute (IPPI), Tehran, Iran
[2] Department of medicinal chemistry, faculty of pharmaceutical chemistry, pharmaceutical sciences branch, Islamic Azad university, Tehran, Iran
[3] Active pharmaceutical ingeredients research center (APIRC), pharmaceutical sciences branch, Islamic Azad university, Tehran, Iran

Received: 2017-06-19 Accepted: 2017-07-15 Published: 2017-08-20

ABSTRACT
Polyacrylic acid/ octavinyl polyhedral oligomeric silsesquioxane, nanocomposite hydrogel with 3-D network was synthesized via radical polymerization. Octavinyl polyhedral oligomeric silsesquioxane was used as crosslinker and nanofiller simultaneously in the preparation of the hydrogel. Hydrogel adsorption performance was determined by adsorption of methylene blue. The adsorption capacity was evaluated under the effects of dye concentration, adsorption contact time and medium pH. The experimental data fitted a pseudo-second-order model and isotherm indicated that the data were agreed with the Langmuir model. The high adsorption capacity (Qmax=1000 (mg/g)) shows the better efficiency of the adsorbent and indicates this hydrogel is a good candidate as the adsorbent of cationic dye and ions.

Keywords: *Organic/inorganic nanocomposite; Hydrogel; Polyacrylic acid; Polyhedral oligomeric silsesquioxane (POSS)*

How to cite this article
Zarezadeh-Mehrizi M, Karimi M, Kalantari khoramdareh Z, Qomi M. Removal of Methylene Blue Using Polyacrylic Acid/Octavinyl Polyhedral Oligomeric Silsesquioxane Nanocomposite. J. Nanoanalysis., 2017; 4(2): 134-141. DOI: 10.22034/jna.2017.02.006

INTRODUCTION

The extensive use of synthetic dyes in many industries such as textile, cosmetic, printing, leather, and petroleum has increased the amount of dye contaminations in the wastewater [1-2]. These dye molecules are mostly non-biodegradable in natural conditions, and some of them *may* be *carcinogenic, mutagenic* and highly toxic on exposed organism. For example, the interaction of cationic dyes with negatively charged cell membrane surfaces can lead to adverse health problems by entering into cells and interacting with cytoplasm [3]. Therefore, the contamination of water resources due to industrial effluents has become one of the world's greatest environmental challenges from a toxicological point of view. However, effective and proper treatment of wastewaters before discharging them into the environment can reduce the residual pollutant contents below the acceptable threshold values impelled by stringent environmental regulations. In recent years, several physical and chemical techniques such as coagulation-flocculation, reverse osmosis, membrane separation, solvent extraction, oxidation-reduction, photo catalysis and adsorption have been examined

* Corresponding Author Email: m.karimi@ippi.ac.ir

to remove dye contaminations from wastewater [1, 4-6]. Among these methods, the adsorption technique is more attractive because of its simplicity of operation, design, high efficiency and low costs. Various adsorbent materials such as activated carbon, zeolite, metal-organic framework, mesoporous silica, synthetic and natural polymers have been studied in the field of wastewater treatment [7-14]. In recent years, the polymeric hydrogels have attracted considerable interest because they can absorb large amounts of water in aqueous solutions due to the considerable amounts of hydrophilic groups in their structures and can remove and trap soluble ions and cationic dyes in an aqueous solution because of the presence of side groups such as amid and carboxylic groups. [15-16]. Recently, various strategies have been investigated to improve the adsorption capacity, mechanical stability and thermal strength of the hydrogels. One of these strategies is the incorporation of nanoparticles in the hydrogel matrix to fabricate organic-inorganic nanocomposite hydrogels. Inorganic nanoparticles such as clay, geraphene oxide, carbon nanotube, montmorillonite, SiO_2, TiO_2 and metallic nanoparticles have been used in pure hydrogel to enhance the hydrogel performance. However, in most reputed works, the nanometers were only, mixed and physically blended within the polymeric matrices which were cross linked with the organic crosslinkers [15, 17-21].

Polyhedral oligomeric silsesquioxanes (POSS) are the smallest existing silica nanoparticles,of about 1-3 nm in size, which have an inorganic rigid core and organic functional groups at each of the eight corners [22]. Multifunctional POSS which are the nanoparticles with more than one reactive organic group can be incorporated into a polymer matrix as a nanostructure and organic crosslinker simultaneously. Covalent bonding between nanoparticles and polymer matrices can improve nanoparticles dispersion in the polymeric matrix and eliminate the macroscopic phase separation between them [23]. Despite this advantage of POSS, there are a few studies that hydrogel cross linked with POSS in order to using as an adsorbent of cationic dye effluents.

In this work, we have used the octavinyl polyhedral oligomeric silsesquioxane nanoparticle (OVS) as a crosslinker for the polyacrylic acid/ OVS hydrogel (PAA/OVS) with 3-D crosslinking network, via radical polymerization. The structure, thermal properties and morphology of PAA/ OVS hydrogel were characterized by FT-IR, DSC and SEM. The adsorption properties of the obtained nanocomposite hydrogel were tested for methylene blue as a model cationic dye. High adsorption capacity with simplicity of design and production of these nanocomposites, in comparison with previously reported works, indicated that polyacrylic acid/octavinyl oligomeric silsesquioxane hydrogel can be used as a good adsorbent of the cationic dye and ions

EXPERIMENTAL

Materials

Vinyltrimethoxysilane (VTMS), hydrochloric acid 37% (HCl), acetone, methanol, dichloromethane, acrylic acid (AA), tetrahydrofuran (THF), methylene blue (MB) and all reagents were obtained from Merck and used without any further purification. N, N'-methylenebisacrylamide (AIBN) was purchased from Aldrich and was used after recrystallization in methanol.

Synthesis of octavinyl polyhedral oligoemric silsesquoxane (OVS)

OVS was prepared according to procedure in the literature [24] . Briefly, 13.4 g VTMS and 135 ml acetone were added into a 500-ml three- necked flask, equipped with a magnetic stirrer, a dropping funnel and a reflux condenser. The solution of 22.5 ml of HCl 37% and 25.9 ml deionized water was added into the reaction mixture and refluxed at 40˚C for 48 h. The white solid product was obtained by filtration and washing with ethanol. The dried product was purified by crystallization from the mixture of three parts of acetone with one of dichloromethane.

Synthesis of PAA/OVS organic-inorganic nanocomposite hydrogel

A hydrogel composed of PAA/OVS was prepared by using acrylic acid (monomer), OVS (crosslinker) and AIBN (initiator) (Figure1). In a 100-mL three-neck flask which was flushed with nitrogen to maintain inert atmosphere, 0.1 g OVS was dissolved in minimum amount of THF (~ 5ml). Then, 2.5 gr (0.035mol) acrylic acid, 0.025 gr AIBN and 10ml THF were simultaneously added into the OVS solution. The mixture was stirred until the AIBN was dissolved completely. After

that, the reaction mixture was kept at 60°C for 6 h to complete polymerization. The synthesized hydrogel was precipitated with water and washed with THF and water several times. The obtained nanocomposites were cut into small pieces and were dried in vacuum at 50°C until their weight remained unchanged.

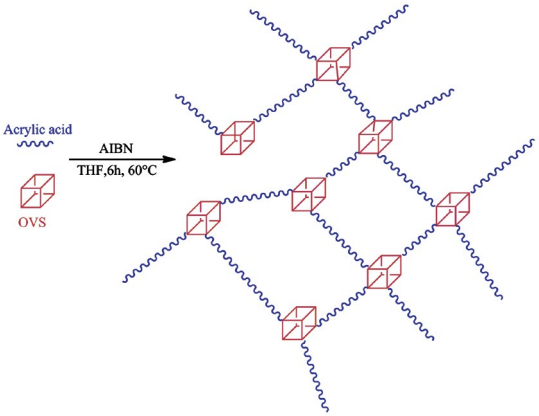

Fig. 1. Schematic representation of the preparation of crosslinked PAA/OVS organic-inorganic nanocomposite hydrogel by radical polymerization.

Dye adsorption onto PAA/OVS hydrogel

Bach adsorption was studied in 25 ml solution of initial dye concentration at room temperature and 0.005 g of the PAA-OVS hydrogel for 24h. To study the effect of pH of MB solution on the adsorption capacity, the pH of the MB solutions adjusted with 0.1 M NaOH or HCl. For kinetic study, 25 ml of dye solution (6-18 $mg.L^{-1}$, without changing the pH) were agitated with 0.005 g of the adsorbent for predetermined intervals of time. Batch equilibrium adsorption was carried out at various dye concentrations of MB solution (24-120 $mg.L^{-1}$) at the pH of the dye solution. The hydrogel was separated from the dye solution by filtration at the predetermined time intervals. The absorbencies of the samples were measured using a UV-vis spectrophotometer (Shimadzo 1650) at wavelength 664 nm for MB.

The adsorption capacity of the adsorbent was calculated using the equilibrium (1):

$$q_e = \frac{(C_0 - C_e)V}{m} \quad (1)$$

Where C_0 is the initial dye concentration in the liquid phase ($mg.L^{-1}$), C_e is the equilibrium concentration of MB ($mg.L^{-1}$), V is the volume of dye solution used (L) and m is the mass of the adsorbent (g).

Characterization

Scanning electron microscopy (SEM) image was taken with a VEGA TESCAN 200 KV (Czech Republic). Fourier transform infrared (FT-IR) spectra of KBr powder-pressed pellets were recorded on an Equinox 55 (Bruker, Germany). ^{1}H and ^{13}C nuclear magnetic resonance spectroscopy (NMR) spectra were recorded on a Bruker 500 and 125 MHz spectrometer in $CDCl_3$, respectively. X-ray powder diffraction (XRD) pattern was taken at a range angle from 5 to 40 degrees by the diffractometer using Cu Kα radiation. The glass transition temperatures (Tg) were determined using a METTLER TOLEDO (Switzerland) scanning calorimeter to perform differential scanning calorimetry (DSC) over a temperature range of 20- 250 °C at a 20 °C/min under nitrogen. Dye concentration was measured by a UV-vis spectrophotometer model Shimadzo 1650 (Japanese).

RESULT AND DISCUSSION

Characterization of the OVS

The crystal structure of the OVS is investigated by XRD analysis. Figure 2 shows the characteristic dominant diffraction peaks at 9.8, 13.0, 19.5, 21.0, 22.8, 23.6, 26.2, 28.2 and 29.6. This pattern indicated that OVS is a highly crystalline material.

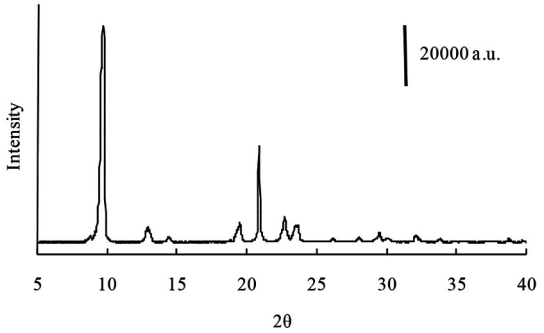

Fig. 2. XRD pattern of the OVS.

OVS was further subjected to NMR measurement. The ^{1}H NMR spectrum of the OVS indicated the multiple absorption band of $Si-CH=CH_2$ at δ~ 6 ppm (Figure 3a.). In the ^{13}C NMR spectrum (Figure 3b), two resonance peaks observed at δ~ 129 and 137 ppm for CH and CH_2, respectively. This document is consistent of the literature [24].

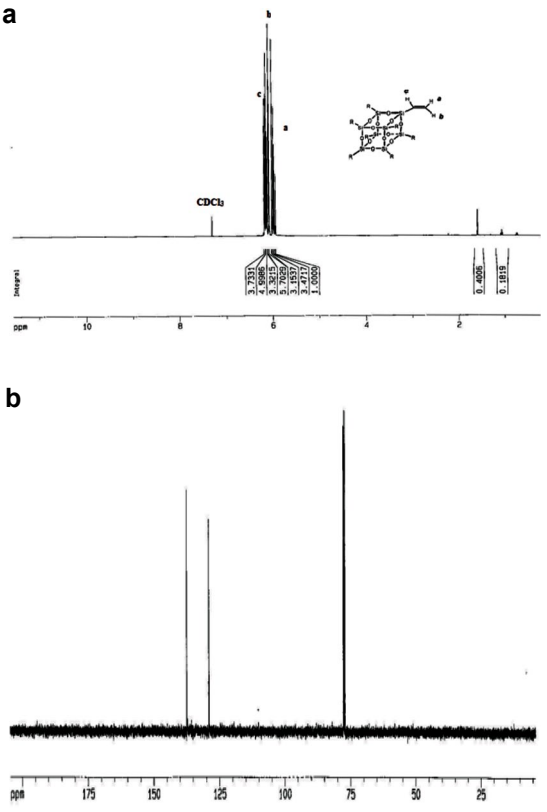

Fig. 3. (a) ^{1}H NMR spectrum and (b) ^{13}C NMR spectrum of the OVS.

The FT-IR spectrum of the OVS is presented in Figure 4. The peaks are assigned as follows: 3010-3070 cm^{-1} (stretching vibration of CH), 1600 cm^{-1} (stretching vibration of C=C), 1410 cm^{-1} (bending vibration of CH_2), 1275 (bending vibration of CH), 1108, 461 cm^{-1} (stretching vibration of SiOSi), 775 cm^{-1} (stretching vibration of Si-C) and 579 cm^{-1} (bending vibration of SiOSi). The bands at 998 and 964 cm^{-1} corresponds to the cage δ (OSiC) deformation modes.

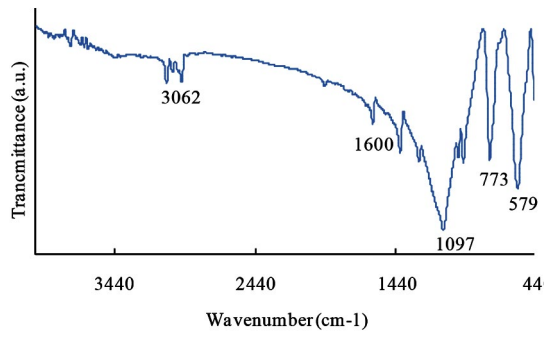

Fig. 4. FTIR spectrum of the OVS.

Characterization of the PAA/OVS hydrogel

SEM images of the PAA/OVS nanocomposit hydrogel are shown in Figure 5a and 5b, before and after swelling in distilled water, respectively. The swollen hydrogel was freeze-dried before SEM analysis. The POSS nanostructures could not be observed in SEM because they have very small sizes (1-3 nm). Figure 5b shows that there are macro-porous and interconnected channels with a uniform pore diameter in the nanocomposite hydrogel. This structure can facilitate the diffusion of the adsorbate, improve the absorption rate of the adsorbent and increase the adsorption capacity. So, it can be concluded that the OVS act as a good crosslinker.

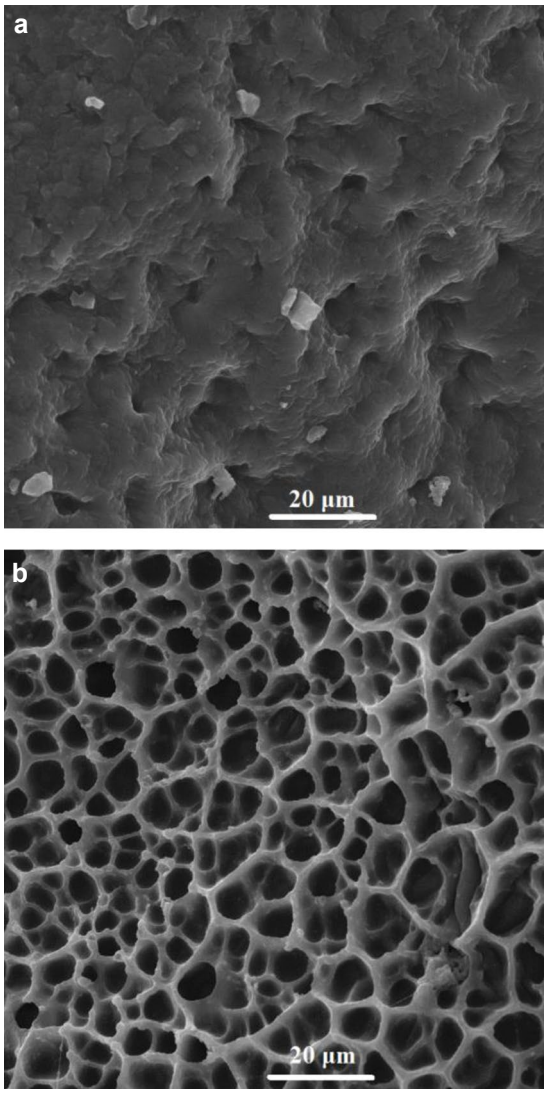

Fig. 5. SEM images of PAA/OVS hydrogel befor (a) and after swelling (b).

DSC curves of the PAA and PAA/OVS hydrogel are shown in Figure 6. The glass transition temperature (Tg) of the PAA and PAA/OVS hydrogel were found to be 44.52 and 46.31 ˚C, respectively. This Tg change is similar phenomena was found in other research [25]. According with this work, the Tg changes is related to the amount of POSS which was incorporated into the nanocomposites. In fact, at low content of POSS, nanoparticles act as a diluent and reduce the Tg of nanocomposite, because of lowering the dipole- dipole interactions. With increase of POSS content and consequently, increase of dipole-dipole interaction of PAA/OVS and POSS/POSS, the Tg of nanocomposits exhibit higher Tg values.

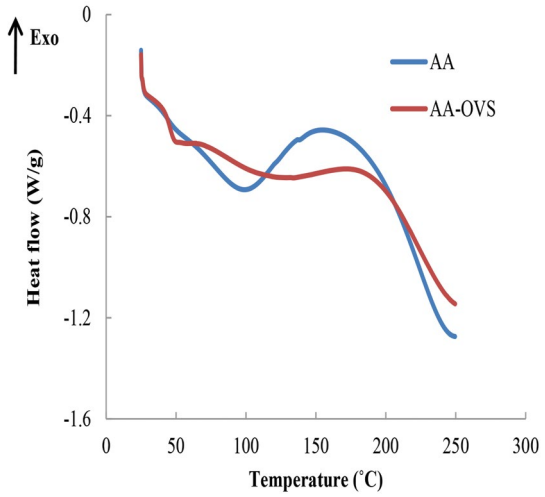

Fig. 6. DSC curves of the AA and AA-OVS hydrogel.

Figure 7 illustrates the FT-IR spectrum of the PAA/OVS hydrogel. A broad peak at 3440 cm^{-1} corresponds to the stretching vibration of hydroxyl groups. The bands appeared at 2917 and 2848 cm^{-1} attributed to the stretching vibration of the CH_2 and CH groups. The PAA shows an intense and broadband at 1722 cm^{-1} related to the C=O groups. The bending vibrations of CH_2 and CH groups are appeared at 1452 and 1403 cm^{-1}[26]. The band at 453, 1108, and 775 cm^{-1} are attributed to the SiOSi of the silsesquioxane cages which illustrate the structure of silsesquioxane is preserved during the polymerization reaction.

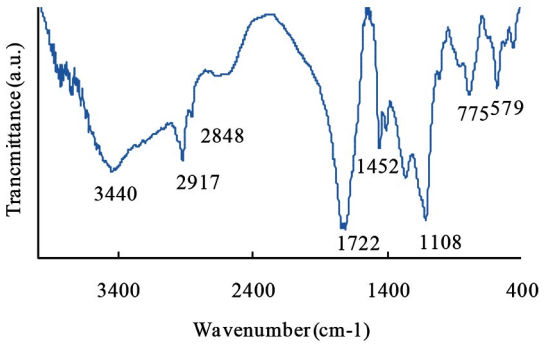

Fig. 7. FTIR spectrum of the PAA/OVS nanocomposite hydrogel.

Adsorption studies

Effect of the pH on the adsorption

The pH of the dye solution has great influence on the adsorption capacity of the adsorbent. The effect of pH dye solution on the PAA/OVS hydrogel was studied and the results are presented in Figure 8. The adsorption capacity of MB increases from 120 to 237 mg. g^{-1} by increasing the pH from 6 to 7. The further increase in the pH has little influence on the adsorption capacity, which remains around 240 mg. g^{-1}. An acidic pH, the hydrogen ion competes with the MB so the adsorption capacity is lower than neutral pH.

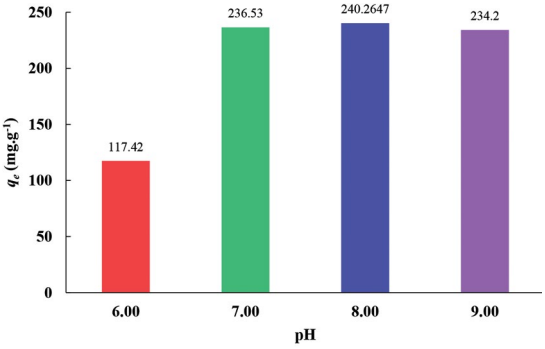

Fig. 8.variation of adsorption capacity of the PAA/OVS hydrogel for MB at different pH (100 mg.L^{-1}).

Adsorption kinetic

Kinetic study is important to investigate the rate as well as the mass transfer mechanism from liquid phase to solid active surface of adsorbent and control the residual time of the whole adsorption process. The effect of contact time on the adsorption capacity of the PAA/OVS hydrogel for MB is shown in Figure 9. The adsorption capacity increases

quickly with the contact time and then reaches the equilibrium. As shown in Figure 9, the increasing trend of q_e in response to time has a low slope value which reflects the porous structure of the hydrogel. The adsorption kinetics were analyzed in order to investigations of the adsorption mechanism of the PAA/OVS hydrogel for MB. The pseudo-first order and pseudo-second order model was used to evaluate the experimental data. The pseudo-first and pseudo-second order kinetic models are shown according to equilibrium 2 and 3, respectively.

$$\log(q_e - q_t) = \log q_e - \frac{k_1 t}{2.303} \quad (2)$$

$$\frac{t}{q_t} = \frac{1}{k_2 q_e^2} + \frac{t}{q_e} \quad (3)$$

Where q_e and q_t (mg. g^{-1}) are the adsorption capacities at equilibrium and at time t, respectively. k_1 and k_2 are the first and second order rate constant, respectively.

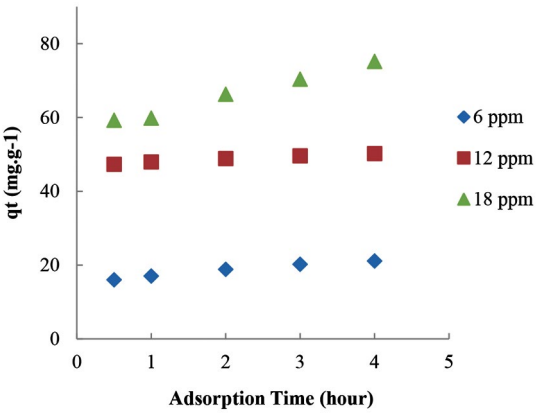

Fig. 9. Effect of contact time on the adsorption capacity.

The values of kinetic studies are listed in table 1. The correlation coefficient for the second order kinetic model (R^2 =0.99) is greater than that of the first order kinetic model (R^2<0.96). Therefore the dye adsorption system is a second order reaction which indicated that MB is most adsorbing onto the adsorbent via chemical interaction [27-28].

Adsorption isotherm

Adsorption isotherm provides evaluation of the distribution coefficient and distribution of solute between the liquid phase and solid phase, information on the nature of the solute-surface interaction and surface properties and affinity of the adsorbent. The adsorption equilibrium was analyzed by Langmuir and Freundlich isotherm models. The adsorption isotherm of MB onto PAA/OVS hydrogel was presented in Figure 10. The affinity between the dye molecules and functional groups on the adsorbent is high as there was sharply increasing of *cue* at a lower equilibrium solution concentration and a plateau shape at a higher equilibrium solution concentration where the adsorption reached in the saturation form. The main consideration of the Langmuir isotherm is that adsorption occurs at the homogeneous adsorption sites. This model can be expressed as follows:

$$\frac{C_e}{q_e} = \frac{1}{b q_m} + \frac{C_e}{q_m} \quad (4)$$

Where C_e (mg.L^{-1}) is the equilibrium concentration of dye and q_e (mg.g^{-1}) is the amount of dye adsorbed per unit mass of adsorbent. q_m denotes the maximum monolayer adsorption capacity. The values of q_m and b are determined from the linear plot of C_e/q_e versus C_e.

Table 1. Kinetic parameters of the adsorption of MB onto PAA/OVS hydrogel obtained using pseudo-first-order and pseudo-second-order model

		Pseudo-first-order			Pseudo-second-order		
C_0	$q_{e,\exp}$	k_1	$q_{e,cal}$		k_2	$q_{e,cal}$	
mg.L^{-1}	mg.g^{-1}	min^{-1}	mg.g^{-1}	R^2	g.mg^{-1}.min^{-1}	mg.g^{-1}	R^2
6	21.40	0.797	9.88	0.951	0.161	22.72	0.999
12	50.31	0.909	6.30	0.900	0.361	52.63	0.999
18	76.75	0.663	31.84	0.958	0.072	83.33	0.998

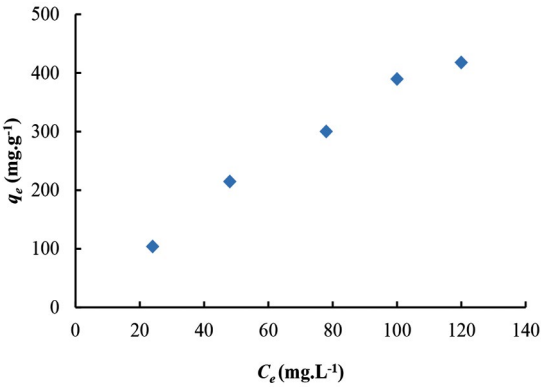

Fig. 10. Effect of initial dye concentration on the adsorption of MB dye by PAA/OVS hydrogel.

A constant separation factor is defined as:

$$R_L = \frac{1}{1 + bC_0} \quad (5)$$

Where C_0 is the initial dye concentration (mg.L^{-1}) and b is related to the energy of the adsorption (L.mg^{-1}). R_L value indicates the variability of the adsorption process. The adsorption process is a favorite ($0<R_L<1$), unfavorable ($R_L> 1$), linear ($R_L=1$) and irreversible ($R_L=0$). The value of R_L is consistent (0.14-0.44) with the favorability of the adsorption process.

Freundlich isotherm is not restricted to the formation of the monolayer. This theory assumes the multilayer adsorption on the heterogeneous surface. The linearized Freundlich equation is given below:

$$\log q_e = \log K_f + (1/n) \log C_e \quad (6)$$

Where q_e and C_e are the absorbent equilibrium concentrations in the solid and liquid phases, respectively. K_f denote Freundlich's uptake factor (adsorption capacity of the adsorbent) and n indicates the variability of the adsorption. The isotherm is favorable when n>1, linear when n=1 and unfavorable when n<1. It was found that the value of n for this isotherm model in this case was greater than 1, indicating that the adsorption of MB onto PAA/OVS hydrogel is favorable. The isotherm constants of these models and the correlation coefficient (R^2) are listed in table 2. By contrasting R^2 values, the Langmuir model fitted better with experimental data.

The adsorption capacity of the PAA/OVS is compared to the other adsorbent and the data given in table 3.

Table 2. Langmuir and Freunlich isotherms parameters for the adsorption of MB onto PAA/OVS

Langmuir model				Freundlich model		
q_m (mg.g^{-1})	b (L.mg^{-1})	R^2	R_L	Kf (mg$^{(n-1)}$/n .g^{-1}. L^{-1})	n	R^2
1000	0.05	0.97	0.14-0.44	69.66	1.89	0.86

Table 3. Comparison of maximum adsorption capacity of different adsorbent for MB

Adsorbent	Adsorption capacity (mg.g^{-1})	References
Hemicellulose-g-ly(methacrylic acid)/ carbon nanotube composite hydrogel	222	[19]
Copolymer of acrylamide and hydroxyethyl methacrylate-POSS	90	[29]
palygorskite/poly(acrylic acid) nanocomposite hydrogels	833	[18]
poly(AA co PVP)/PGS composite	1815	[20]
PAA/OVS nanocomposite hydrogel	1000	This work

It can be concluded that PAA-OVS can be used as an adsorbent for the removal of cationic dye such as MB.

CONCLUSION

The PAA/OVS organic/inorganic nanocomposite hydrogel (PAA/OVS) with the 3-D crosslinking network was synthesized using OVS as a crosslinking agent and nanostructure, via radical polymerization. The PAA/OVS hydrogel was used for the removal of MB from aqueous solution. The Langmuir model with the monolayer adsorption capacity of 1000 $mg.g^{-1}$ was the best isotherm model describing the experimental data. The adsorption kinetics were agreed well with the pseudo-second-order model. PAA/OVS nanocomposite hydrogels with high adsorption capacity and simplicity of design provide high noteworthy application prospects in wastewater treatments and indicate that the multifunctional POSS organic/ inorganic nanostructures are a suitable candidate for use in hydrogels as a crosslinker.

ACKNOWLEDGMENT

The authors gratefully thank Iran Polymer and Petrochemical Institute (IPPI) for supporting of this work.

CONFLICT OF INTEREST

The authors declare that there is no conflict of interests regarding the publication of this manuscript.

REFERENCES

1. M. Rafatullah, O. Sulaiman, R. Hashim and A. Ahmad, Journal of Hazardous Materials, 177, 70 (2010).
2. R. Bhattacharyya and S.K. Ray, Chemical Engineering Journal, 260, 269 (2015).
3. C. Zhou, Q. Wu, T. Lei and I.I. Negulescu, Chemical Engineering Journal, 251, 17 (2014).
4. H. Mittal, A. Maity and S.S. Ray, Chemical Engineering Journal, 279, 166 (2015).
5. D. Chen, Z. Zeng, Y. Zeng, F. Zhang and M. Wang, Water Resources and Industry, 15, 1 (2016).
6. M.T. Yagub, T.K. Sen, S. Afroze and H.M. Ang, Advances in Colloid and Interface Science, 209, 172 (2014).
7. Q. Zhao and T. Cao, Industrial & Engineering Chemistry Research, 51, 4952 (2012).
8. E. Fois, G. Tabacchi, A. Devaux, P. Belser, D. Brühwiler and G. Calzaferri, Langmuir, 29, 9188 (2013).
9. V.O. Njoku, K.Y. Foo, M. Asif and B.H. Hameed, Chemical Engineering Journal, 250, 198 (2014).
10. H. Chaudhuri, S. Dash and A. Sarkar, Industrial & Engineering Chemistry Research, 55, 10084 (2016).
11. E. Haque, J.W. Jun and S.H. Jhung, Journal of Hazardous Materials, 185, 507 (2011).
12. D. Parasuraman and M.J. Serpe, ACS Applied Materials & Interfaces, 3, 4714 (2011).
13. R. Vodă, L. Lupa, A. Negrea, M. Ciopec, P. Negrea and C.M. Davidescu, Separation Science and Technology, 51, 2511 (2016).
14. A.U. Khan, Y. Wei, Z.U. Haq Khan, K. Tahir, A. Ahmad, S.U. Khan, F.U. Khan, Q.U. Khan and Q. Yuan, Separation Science and Technology, 51, 1070 (2016).
15. S. Thakur, S. Pandey and O.A. Arotiba, Carbohydrate Polymers, 153, 34 (2016).
16. M.A. Mekewi, T.M. Madkour, A.S. Darwish and Y.M. Hashish, Journal of Industrial and Engineering Chemistry, 30, 359 (2015).
17. H. Ge and J. Wang, Chemosphere, 169, 443 (2017).
18. L. Zhu, J. Guo, P. Liu and S. Zhao, Applied Clay Science, 121–122, 29 (2016).
19. X.-F. Sun, Q. Ye, Z. Jing and Y. Li, Polymer Composites, 35, 45 (2014).
20. C.-x. Yang, L. Lei, P.-x. Zhou, Z. Zhang and Z.-q. Lei, Journal of Colloid and Interface Science, 443, 97 (2015).
21. S.R. Shirsath, A.P. Patil, R. Patil, J.B. Naik, P.R. Gogate and S.H. Sonawane, Ultrasonics Sonochemistry, 20, 914 (2013).
22. D.B. Cordes, P.D. Lickiss and F. Rataboul, Chemical Reviews, 110, 2081 (2010).
23. E. Ayandele, B. Sarkar and P. Alexandridis, Nanomaterials, 2, 445 (2012).
24. D. Chen, S. Yi, W. Wu, Y. Zhong, J. Liao, C. Huang and W. Shi, Polymer, 51, 3867 (2010).
25. H. Xu, B. Yang, J. Wang, S. Guang and C. Li, Macromolecules, 38, 10455 (2005).
26. M.A. Moharram, S.M. Rabie and H.M. El-Gendy, Journal of Applied Polymer Science, 85, 1619 (2002).
27. T.A. Saleh, A.M. Muhammad, B. Tawabini and S.A. Ali, Journal of Chemical & Engineering Data, 61, 3377 (2016).
28. Y. Li, M. Wu, B. Wang, Y. Wu, M. Ma and X. Zhang, ACS Sustainable Chemistry & Engineering, 4, 5523 (2016).
29. A. Akbari and N. Arsalani, Polymer-Plastics Technology and Engineering, 55, 1586 (2016).